Photoelastic modulated imaging ellipsometry by stroboscopic illumination technique

Chien-Yuan Han and Yu-Faye Chao

Citation: Review of Scientific Instruments **77**, 023107 (2006); doi: 10.1063/1.2173027
View online: http://dx.doi.org/10.1063/1.2173027
View Table of Contents: http://scitation.aip.org/content/aip/journal/rsi/77/2?ver=pdfcov
Published by the AIP Publishing

Articles you may be interested in
Deassociate the initial temporal phase deviation provided by photoelastic modulator for stroboscopic illumination polarization modulated ellipsometry
Rev. Sci. Instrum. **82**, 035117 (2011); 10.1063/1.3568745

Coherent detection of nonlinear nanomechanical motion using a stroboscopic downconversion technique
Appl. Phys. Lett. **94**, 263104 (2009); 10.1063/1.3155164

Generalized theory and application of Stokes parameter measurements made with a single photoelastic modulator
J. Appl. Phys. **100**, 063537 (2006); 10.1063/1.2353894

Characterization of thin SiO 2 on Si by spectroscopic ellipsometry, neutron reflectometry, and x-ray reflectometry
AIP Conf. Proc. **449**, 185 (1998); 10.1063/1.56796

Thin film ellipsometry metrology
AIP Conf. Proc. **449**, 121 (1998); 10.1063/1.56787

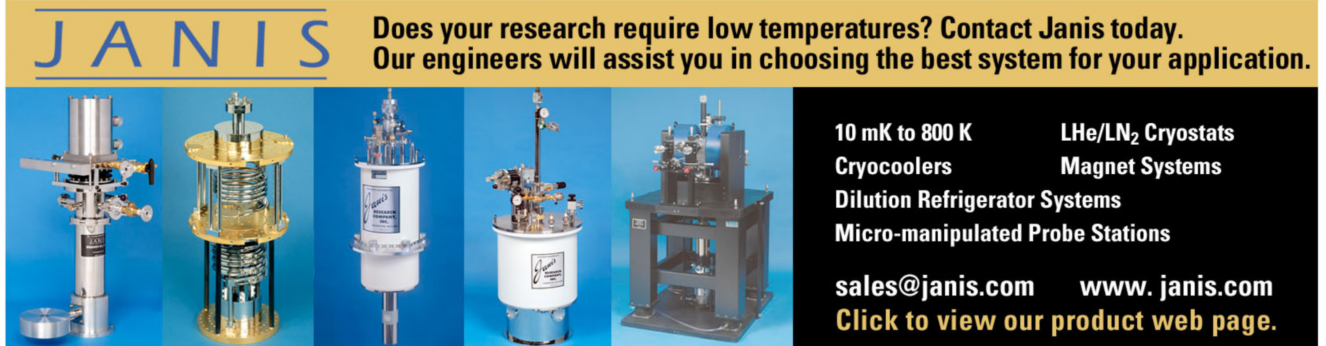

This article is copyrighted as indicated in the article. Reuse of AIP content is subject to the terms at: http://scitationnew.aip.org/termsconditions. Downloaded to IP: 140.113.38.11 On: Thu, 01 May 2014 02:09:26

Photoelastic modulated imaging ellipsometry by stroboscopic illumination technique

Chien-Yuan Han and Yu-Faye Chao
Department of Photonics, Institute of Electro-optical Engineering, National Chiao Tung University, 1001 Ta Hsueh Road, Hsinchu 300, Taiwan

(Received 13 October 2005; accepted 12 January 2006; published online 24 February 2006)

A novel stroboscopic illumination technique is applied in a photoelastic modulated (PEM) ellipsometry to conquer the slow imaging processing of charge-coupled device camera system and form a fast imaging ellipsometry. The synchronized ultrastable short pulse is used to freeze the intensity variation of the PEM modulated signal. The temporal phase is calibrated with respect to the time reference of PEM. The laser diode is modulated by a programable pulse generator for triggering four short pulses at their specific temporal phase angle. The two-dimensional (2D) ellipsometric parameters can be deduced from those recorded four images. Therefore, the 2D thickness profile of a patterned sample can be measured; a static patterned SiO_2 thin film on silicon substrate and the drainage behavior of matching oil on silicon wafer were studied by this imaging ellipsometry. © *2006 American Institute of Physics.* [DOI: 10.1063/1.2173027]

INTRODUCTION

Ellipsometry is a widely used optical technique for thin film measurements because it offers a nondestructive way to accurately determine the film thickness and optical constants.[1] In the recent development of thin film fabrication, the *in situ* ellipsometric method becomes an indispensable technique for monitoring the film growth/etching in order to meet the requirement of the ever-increasing complexity of thin film structure.[2] Moreover, ellipsometry also plays an important role in investigating the interfacial dynamics by combining the surface plasmon resonance technique through a prism.[3] It has been reported that one can either study the dynamic properties by single point detection or study the static property of a surface by imaging ellipsometry. Normally, the imaging ellipsometry is realized by scanning[4] or using a digital camera in the rotating element[5] ellipsometry, all of them containing at least one mechanical moving part, which not only slows down but also degrades the accuracy of its measurement, because the moving part can cause the beam to deviate[6] and produce parasitic errors.

The most prevalent real-time monitoring ellipsometer is the photoelastic modulated (PEM) type, which operates at high frequency (most of them are at 50 kHz) with no moving part. For single spot detection, either lock-in amplifier[7] or data acquisition system[8] is used to obtain the ellipsometric parameters by a fast response detector; neither of these configurations is suitable for a two-dimensional measurement because the data-acquiring speed of charge-coupled device (CCD) camera is too slow to obtain the temporal variation of PEM. To overcome this deficiency, we replace the conventional detection method by synchronizing the ultrastable short pulse to freeze the intensity variation of the PEM signal.[9] The pulse current for driving the laser diode is controlled by a programable pulse generator; while the temporal reference is provided by the controller of PEM. The ellipsometric parameters can be determined by converting the measured intensity at four specific temporal phases. Since the precision of temporal phase is crucial to the measurement of ellipsometric parameters, we calibrate the reference zero of time by a premeasured platinum film on silicon substrate. In addition to the thickness profile of the patterned SiO_2 thin film on silicon substrate, we also measured the drainage behavior of matching oil on silicon wafer by this imaging ellipsometry.

THEORY

Ellipsometry measures the changes of the polarization states of the light reflected from the sample surface to deduce its optical parameters, such as refraction indices or layer thickness. The ellipsometry basically measures two parameters, Ψ and Δ, which are defined as

$$\tan \Psi e^{i\Delta} = \frac{r_p}{r_s}, \tag{1}$$

where r_p and r_s are the complex Fresnel reflection coefficients for the polarized light parallel and perpendicular to the plane of incidence, respectively. We replace the compensator by a PEM in the polarizer-compensator-sample-analyzer (PCSA) setup. The final polarization state can be expressed by the operation of their corresponding Mueller matrices, i.e.,

$$S_f = M_A(A) R_S(\Psi,\Delta) M_{\text{PEM}}(\Delta_P) S_P, \tag{2}$$

where the Stokes vector S_f is the final polarization state of the reflected light, the Stokes vector S_P denotes the initial linearly polarized light at the azimuth angle of P, $M_{\text{PEM}}(\Delta_P)$ represents the Mueller matrix of the PEM, whose azimuth of its optical axis is zero with respect to the incident plane with a modulated phase Δ_P, $R_S(\Psi,\Delta)$ represents the Mueller matrix of the sample whose ellipsometric parameters are Ψ and Δ, and $M_A(A)$ is the Mueller matrix of an analyzer with its transmission axis at the azimuth angle of A. If $P=-45°$ and

 © 2006 American Institute of Physics

This article is copyrighted as indicated in the article. Reuse of AIP content is subject to the terms at: http://scitationnew.aip.org/termsconditions. Downloaded to IP: 140.113.38.11 On: Thu, 01 May 2014 02:09:26

$A=45°$, the temporally reflected intensity can be proven to be

$$I(t) = \frac{I_0}{2}[1 + \sin 2\Psi \cos(\Delta - \Delta_p)], \quad (3)$$

where I_0 is the normalized intensity of the system. The phase retardation (Δ_P) of the PEM is modulated as $\delta_0 \sin \omega t$. If the amplitude of modulation (δ_0) is π, one can formulate the temporal intensity behavior as

$$I(t) = \frac{I_0}{2}[1 + \sin 2\Psi \cos(\Delta - \pi \sin \omega t)]. \quad (4)$$

When the temporal phase angles ωt are 0° and 90°, the corresponding intensities can be expressed as

$$I_{0°} = \frac{I_0}{2}[1 + \sin 2\Psi \cos \Delta]$$

and

$$I_{90°} = \frac{I_0}{2}[1 - \sin 2\Psi \cos \Delta],$$

respectively. It is easy to prove that

$$\sin 2\Psi \cos \Delta = \frac{I_{0°} - I_{90°}}{I_{0°} + I_{90°}} = I'. \quad (5)$$

Using the similar process for ωt at 30 and 210°, one can obtain

$$\sin 2\Psi \sin \Delta = \frac{I_{30°} - I_{210°}}{I_{30°} + I_{210°}} = I''. \quad (6)$$

Thus, the ellipsometric parameters can be determined by measuring the intensity at these four temporal phases, as follows

$$\Delta = \tan^{-1}\left(\frac{I''}{I'}\right); \quad (7)$$

$$\Psi = \frac{1}{2} \sin^{-1}(\sqrt{I'^2 + I''^2}). \quad (8)$$

The time-varying signal can be frozen at these points by illuminating the objects with short synchronized stroboscopic pulses.

To drive the laser diode, the short-current pulses are precisely controlled by a programable pulse generator, whose reference is triggered by the PEM for synchronizing stroboscopic illumination. We choose the exposure time Δt of the CCD camera to be a few tens of a second for maintaining the intensity in linear range. Since the modulation frequency of PEM is 50 kHz, the camera will integrate the flux over N $(\Delta t \times 50\,000)$ pulses (e.g., $\Delta t=0.1$ s, $N=5000$) at a fixed temporal phase during exposure.[10] The concept of stroboscopic illumination is illustrated in Fig. 1; the temporal wave form of the reflected light in this PEM ellipsometer is obtained by taking these four specific temporal phases to be stroboscopically illuminated.

SYSTEM CONFIGURATIONS

The schematic configuration of this stroboscopic illumination imaging ellipsometry is set up as shown in Fig. 2. The basic structure of this imaging ellipsometry is a phase modulated ellipsometry: its light source is a pulse modulated laser diode (HITACHI, HL6501MG) for stroboscopic illumination; its phase is modulated by a PEM (Hinds PEM90/CF50); and its beam is expanded (Galilean beam expander, ×7) and detected by a CCD camera (Starlight MX516) for imaging process. The optical axis of PEM and the transmission axes of two linear polarizers are well aligned to the incident plane according to Ref. 11. The amplitude of PEM modulation is set to be π. The modulated pulse is achieved by a dc bias current equal to the threshold value coupled with a programable pulse generator (HP 8110A) to drive the laser diode. A square wave provided by the PEM can be used to trigger the four specific temporal phases (0°, 30°, 90°, and 210°) for the stroboscopic illumination with a pulse width of 108 ns (~2° phase change of modulator). The exposure time of the CCD camera (512×290 pixels with a 16 bit gray scale) is set to be a few tens of a second for maintaining enough intensity in its linear range.

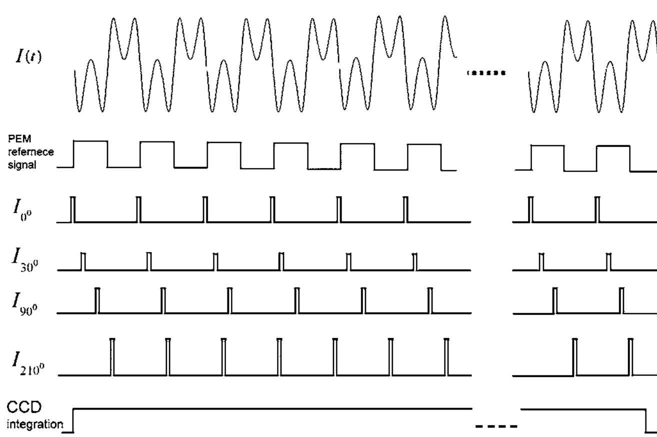

FIG. 1. Principle of image acquisition: each frame $(I_{0°}, I_{30°}, I_{90°}, I_{210°})$ results from the accumulation by N short pulses of the modulated signal $I(t)$ at the specific phase angle in the exposure time of CCD. The four frames are acquired in sequence by the synchronized ultra stable short-pulse illumination. The ellipsometric images are calculated by these four frames.

CALIBRATION OF THE TEMPORAL PHASE DELAY

Since it is crucial to trigger the strobe at the right temporal phase in this stroboscopic illumination ellipsometry, we

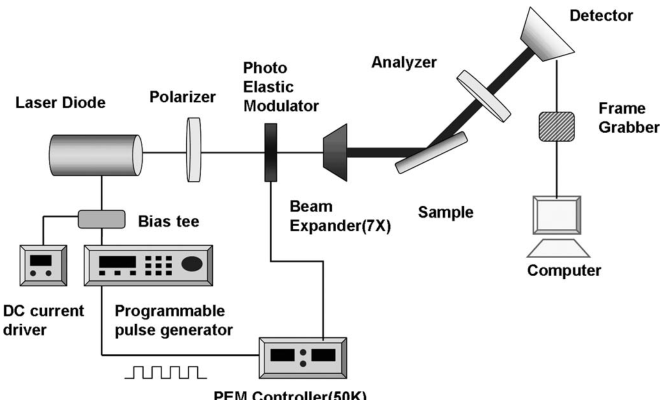

FIG. 2. Experimental setup of the photoelastic modulated imaging ellipsometry by stroboscopic illumination technique.

This article is copyrighted as indicated in the article. Reuse of AIP content is subject to the terms at: http://scitationnew.aip.org/termsconditions. Downloaded to IP: 140.113.38.11 On: Thu, 01 May 2014 02:09:26

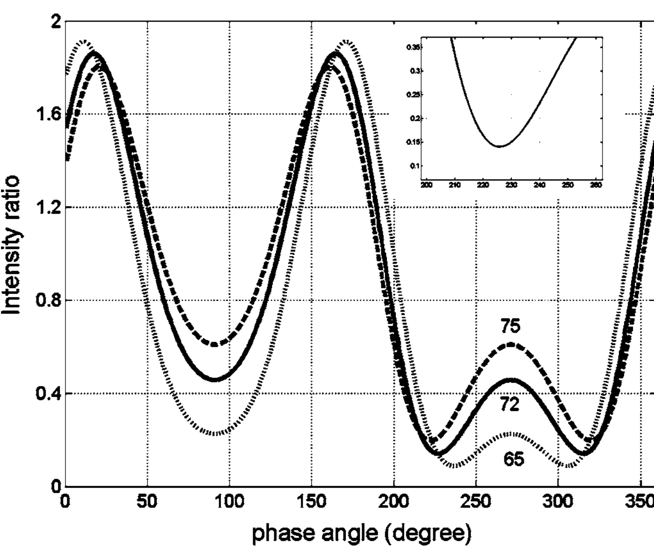

FIG. 3. The numerically simulated temporal wave forms of Pt/Si are at the incident angles of 65°, 72°, and 75°. Insert: The enlarged wave form at the incident angle of 72°; its local minimum intensity is at 226°.

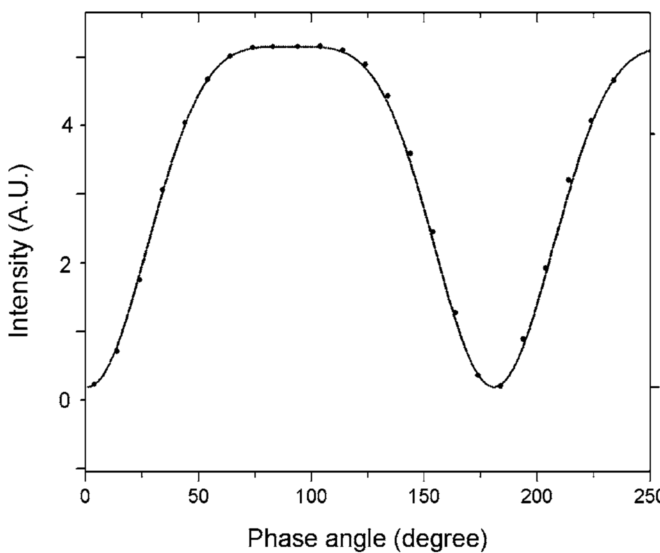

FIG. 5. The wave form of a transmitted mode: the solid line represents the theoretical intensity curve and the data points are the measured intensity at the phase angle.

analyzed the temporal phase of two photoelastic modulators (PEM80 and PEM90) with their self-provided reference zero under the *P*-PEM-*A* transmitted configuration and set both of their modulation amplitudes at π we found that one of reference zeros do not match with the initial phase of its modulation signal.[12] Since the temporal wave form of the half-wave modulated PEM has a twofold symmetry in the transmission mode,[11] we deliberately chose an optically thick platinum film on silicon substrate (Pt/Si) to identify the temporal phase delay of the reference zero in the PEM ellipsometry. Because of the inert metallic property of Pt and our previous study,[13] the ellipsometric parameters of Pt/Si of an optically thick platinum film (much thicker than the skin depth; it can be considered as infinitely thick) are very stable in air, so we numerically analyzed the digital temporal wave forms (TW) of Pt/Si in PEM ellipsometry under various angles of incidence at the wavelength of 660 nm. The asymmetric distribution of the TW, as shown in Fig. 3, can be used to locate the phase delay of its reference zero. Then, we set up a similar ellipsometric configuration to locate the local minimum intensity of the TW at the same temporal phase with the reference zero by varying the incident angle. After adjusting the incident angle to 72°, we observed that the local minimum of the TW coincided with reference zero in the oscilloscope (Tektronix TDS 784), as in Fig. 4. Ψ (29.63°) and Δ (230.84°) were measured by the conventional PEM ellipsometry[12] under the same conditions, and then their values were substituted into Eq. (1). One can easily obtain the phase delay, which is 226°, by zooming in its TW curve, as shown in the insert of Fig. 3. After the phase delay of the reference zero was determined, we proceed with the experiment to confirm this calibration by measuring the TW in the *P*-PEM-*A* transmission setup. By adjusting the tempo-

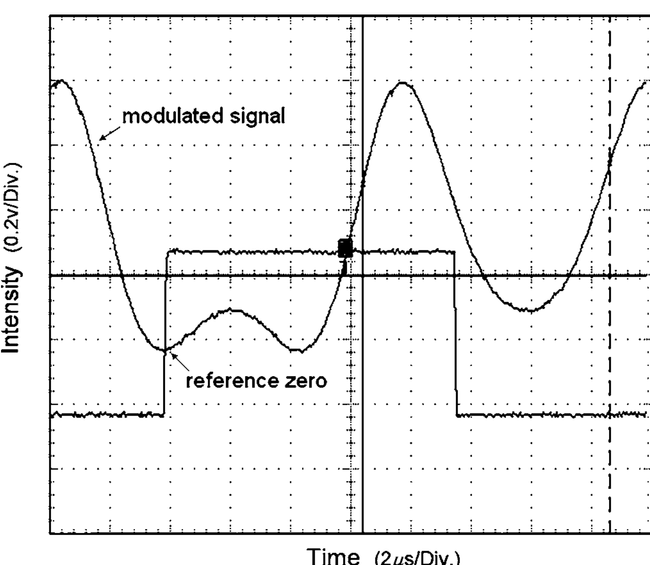

FIG. 4. The temporal wave forms of the Pt/Si thin film and the reference square wave provided by the PEM; the local minimum intensity does match with the reference zero. The premeasured Ψ and Δ are 29.63° and 230.84°, respectively, under the incident angle of 72°.

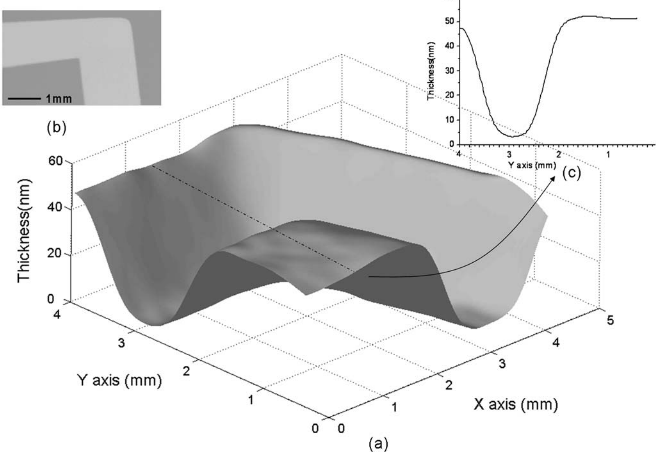

FIG. 6. The L shaped SiO_2 layer: (a) the two-dimensional thickness profile, (b) the photo image, and (c) the thickness profile of the SiO_2 film at X =1.5 mm.

This article is copyrighted as indicated in the article. Reuse of AIP content is subject to the terms at: http://scitationnew.aip.org/termsconditions. Downloaded to IP: 140.113.38.11 On: Thu, 01 May 2014 02:09:26

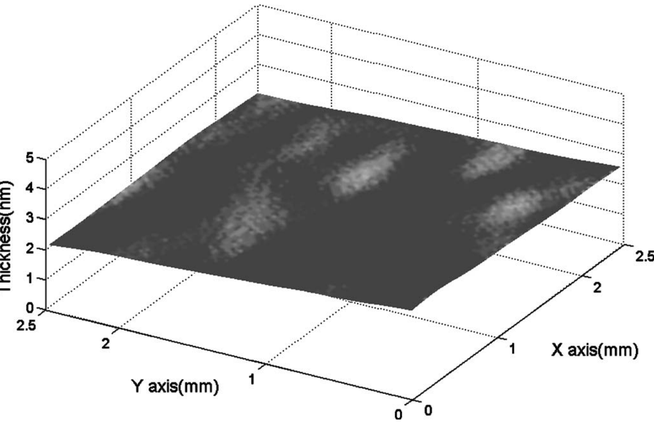

FIG. 7. Thickness profile of the bare silicon wafer: oxide thickness is 2.4±0.2 nm.

ral zero to be at 226° and then choosing the intensity of the brightest pixel in the image area, we measured the intensity from 0° to 240° with a step of 10° and compared with the theoretical intensity distribution, as depicted in Fig. 5. This not only confirms the phase delay of the reference zero, it also demonstrates the linearity response of the CCD camera system with respect to the strobe light of laser diode.

EXPERIMENTAL PROCEDURES

To examine the accuracy of this stroboscopic illumination imaging ellipsometry, the two-dimensional thickness distribution of a patterned SiO_2 film on silicon substrate (SiO_2/Si) was determined. The photolithographic technique and buffered oxide etch (BOE, $NH_4F/HF/H_2O$) wet etching

FIG. 8. The drainage process of an oil droplet: (a) the two-dimensional distribution of Δ for every 30 s, (b) Δ distribution of the cross section through the center of the oil droplet at $t=60$ s, and (c) the thickness profile of the cross section through the center of the oil droplet at $t=60$ s.

This article is copyrighted as indicated in the article. Reuse of AIP content is subject to the terms at: http://scitationnew.aip.org/termsconditions. Downloaded to IP: 140.113.38.11 On: Thu, 01 May 2014 02:09:26

were used to create an L shaped pattern on a 50 nm thick SiO_2 layer on silicon substrate. It is notable that the BOE solution has a typical etching rate of 100 nm/min, and 1 min etching time was used in this work. The 8 mm diameter expanded beam was used to investigate an area of 3.75 $\times 5$ mm^2 at the corner of this L shaped pattern. After the alignment and calibration of the optical system, we sequentially took four images at the temporal phases of 0°, 30°, 90°, and 210°. In addition to the static measurement, we performed the similar imaging process for an oil droplet on a vertical bare silicon surface. Since the microscopic index matching oil (Nikon, n_d=1.515) is highly viscous on the silicon surface, we chose the oil droplet to be our dynamic sample in this imaging ellipsometry. The oil droplet on the vertical bare silicon surface was probed by the PEM ellipsometry under the incident angle of 70°. The size of the oil droplet is 2 μl, which is the smallest quantity of the microliter pipette; the oil droplet was dropped off from the top of this vertically held silicon wafer. Since the exposure time (0.2 s) for a frame plus the time required to transfer charge (3 s) from the image region to the store region of each image in the CCD camera system is 3.2 s, the total acquisition time of one set of ellipsometric parameters is about 13 s, because there are four images in one set. Six sets of ellipsometric parameters were obtained in the oil dropping process. Because the CCD camera system has not been integrated with the stroboscopic illumination system, a time interval of 17 s between two consecutive imaging processes was used for manually controlling the synchronization. The whole oil dropping process was completed in 2.5 min.

RESULTS

The thickness profile of the L patterned SiO_2/Si thin film was deduced from the measured ellipsometric parameters, as shown in Fig. 6. The thickness on the plateau of the profile is about 52 nm, which is consistent with the thickness before etching. Because we neglected the static phase retardation of PEM, which is about 2°, the 2 nm oxide layer was measured as 3 nm after etching, shown in the insert of Fig. 6. Moreover, we set the beam expander in front of the sample, which dramatically reduced the optical resolution, the round-off at the corner and no flat area after etching are also under our expectation. Before dropping off the oil on the silicon surface, we deduced the thickness of SiO_2 film to be 2.4±0.2 nm, as shown in Fig. 7; a slight tilting of the surface can also be observed. Since the reflectance of a flat surface is much higher than that of a rough surface, the exposure time has to be carefully chosen for studying the oil dropping in order to avoid the over exposure in the flat area of the wafer. For the same reason, we were unable to obtain an accurate measurement of Ψ, which is the main disadvantage of the PEM ellipsometry. In measuring the motion of the tip of the oil droplet, we conclude that the dropping speed of the oil droplet is 20 μm/s, as shown in Fig. 8. Because we do know the refractive index of the matching oil, it is able to deduce the line profile at the cross section by simply using the ellipsometric parameter Δ along the tip of the oil droplet at t=60 s, as shown in Fig. 8. By fitting the film model of air/oil/SiO_2 (2.4 nm)/Si to the measurement of Δ, we obtained the tip height of the oil droplet to be about 5.2 nm.

DISCUSSION

Applying the stroboscopic illumination technique in PEM ellipsometry can reduce the acquisition time in imaging ellipsometry. The fastest imaging ellipsometry known is in the order of minutes, while the time resolution of this PEM imaging ellipsometry is limited by the rate of frame grabbing of the CCD camera system. The frame rate in our system is 0.3 fps, but it is not integrated with the programable pulse generator. We can double the speed if the system was integrated and synchronized with the pulse generator. One can also reduce the imaging process by reducing the exposure time of the CCD camera, which requires a dark background and increased power of laser. The lateral interference has been studied[14] in the etching process of patterned film by single spot; it will be a great merit by *in situ* study using this dynamic imaging ellipsometry.

This is a preliminary study of stroboscopic technique in ellipsometry; the systematic errors, such as the intrinsic phase retardation of the PEM and misalignment of the optical components and depolarization effect, are completely ignored. For improving the lateral resolution of this imaging ellipsometry, we not only have to solve the system errors, we also have to solve the polarization aberration caused by the beam expansion.

ACKNOWLEDGMENTS

This work is supported by National Science Council (NSC) in Taiwan under Grant No. NSC 94-2215-E-009-015. The authors are grateful to Jiun-Rung Lin for preparing the patterned SiO_2 thin film on silicon substrate.

[1] R. M. Azzam and N. M. Bashara, *Ellipsometry and Polarized Light* (North Holland, Amsterdam, 1979).
[2] G. E. Jellison, Jr., Thin Solid Films **313–314**, 33 (1998).
[3] P. Westphal and A. Bornmann, Sens. Actuators B **84**, 278 (2002).
[4] A. H. Liu, P. C. Wayner, Jr., and J. L. Plawsky, Appl. Opt. **33**, 1223 (1994).
[5] Beaglehole instruments, http://www.beaglehole.com
[6] M. W. Wang, Y. F. Chao, and Z. C. Ko, J. Phys. D **32**, 2246 (1999).
[7] S. N. Jasperson and S. E. Schnatterly, Rev. Sci. Instrum. **40**, 761 (1969).
[8] M. W. Wang, F. H. Tsai, and Y. F. Chao, Thin Solid Films **455–456**, 78 (2004).
[9] A. Dubois, L. Vabre, A. C. Boccara, and E. Beaurepaire, Appl. Opt. **41**, 805 (2002).
[10] P. Gleyzes, A. C. Boccara, and H. Saint-Jalmes, Opt. Lett. **22**, 1529 (1997).
[11] M. W. Wang, Y. F. Chao, and S. Liu, Jpn. J. Appl. Phys., Part 1 **38**, 6919 (1999).
[12] M. W. Wang, Y. F. Chao, K. C. Leou, F. H. Tsai, T. L. Lin, S. S. Chen, and Y. W. Liu, Jpn. J. Appl. Phys., Part 1 **43**, 827 (2004).
[13] Y. F. Chao, W. C. Lee, C. S. Hung, and J. J. Lin, J. Phys. D **32**, 2246 (1999).
[14] S.-J. Cho, P. G. Snyder, C. M. Herzinger, and B. Johs, J. Vac. Sci. Technol. B **20**, 197 (2002).

This article is copyrighted as indicated in the article. Reuse of AIP content is subject to the terms at: http://scitationnew.aip.org/termsconditions. Downloaded to IP: 140.113.38.11 On: Thu, 01 May 2014 02:09:26